

Immunomodulatory oligonucleotides as novel therapy for breast cancer: pharmacokinetics, *in vitro* and *in vivo* anticancer activity, and potentiation of antibody therapy

Hui Wang,^{1,2} Elizabeth R. Rayburn,¹ Wei Wang,¹ Ekambar R. Kandimalla,⁴ Sudhir Agrawal,⁴ and Ruiwen Zhang^{1,2,3}

¹Department of Pharmacology and Toxicology, Division of Clinical Pharmacology; ²Comprehensive Cancer Center; and ³Gene Therapy Center, University of Alabama at Birmingham, Birmingham, Alabama; and ⁴Idera Pharmaceuticals, Inc., Cambridge, Massachusetts

Abstract

Oligonucleotides containing CpG motifs and immunomodulatory oligonucleotides (IMO) containing a synthetic immunostimulatory dinucleotide and a novel DNA structure have been suggested to have potential for the treatment of various human diseases. In the present study, a newly designed IMO was evaluated in several models of human (MCF-7 and BT474 xenograft) and murine (4T1 syngeneic) breast cancer. Pharmacokinetics studies of the IMO administered by s.c., i.v., p.o., or i.p. routes were also accomplished. The IMO was widely distributed to various tissues by all four routes, with s.c. administration yielding the highest concentration in tumor tissue. The IMO inhibited the growth of tumors in all three models of breast cancer, with the lowest dose of the IMO inhibiting MCF-7 xenograft tumor growth by >40%. Combining the IMO with the anticancer antibody, Herceptin, led to potent antitumor effects, resulting in >96% inhibition of tumor growth. The IMO also exerted *in vitro* antitumor activity, as measured by cell growth, apoptosis, and proliferation assays in the presence of Lipofectin. This is the first report of the pharmacokinetics of this agent in

normal and tumor-bearing mice. Based on the present results, we believe that the IMO is a good candidate for clinical development for breast cancer therapy used either alone or in combination with conventional cancer therapeutic agents. [Mol Cancer Ther 2006;5(8):2106–14]

Introduction

It is estimated that almost 41,000 women in the United States will die from breast cancer this year (1). One in eight American women will develop the disease at some point during their life (2). Although early detection of breast cancer has improved both through advances in technology and through better education, the mortality rate has dropped only slightly in the past few years (3). There have also been some improvements in the treatment of breast cancer and prevention of recurrence through use of antiestrogens, such as tamoxifen. These drugs have provided new hope for patients, but their use can result in an increase in other types of cancer, such as uterine cancer, and long-term treatment can lead to resistance (4, 5). New therapies are urgently needed to make an impact on the survival of patients. Immunotherapy has great potential for the treatment of breast cancer, with monoclonal antibodies already being used in the clinic (6).

As one of the novel immunotherapy approaches, oligonucleotides containing CpG motifs have attracted intensive investigations. As early as the 1980s, it was known that certain DNA sequences and synthetic oligonucleotides could induce type 1 IFNs and natural killer cell activity, and had antitumor activity (7–10). These activities of bacterial and synthetic DNA are related to the presence of unmethylated CpG motifs within their sequences. CpG DNA acts as a pathogen-associated molecular pattern molecule, mimicking a bacterial infection, and is recognized by Toll-like receptor 9 (TLR9; refs. 11, 12). Recognition of CpG DNA by TLR9 activates a signaling cascade leading to the activation of NF- κ B and activator protein-1 pathways (13). This immune stimulation results in the production of cytokines and chemokines, which increase B-cell proliferation, macrophage activation, natural killer cell activity, and dendritic cell maturation, differentiation, and migration (14–19). CpG DNA has shown efficacy in the treatment of cancer and various other diseases (20–24). Several potential mechanisms of anticancer action exist. These include the enhancement of immune surveillance, a decrease in tumor energy, and changes in the tumor microenvironment (25).

There is ample evidence supporting a structure-activity relationship for immunostimulatory and immunomodulatory oligonucleotides (IMO; 26–36). The presence of a CpG

Received 3/22/06; revised 5/18/06; accepted 6/15/06.

Grant support: A research agreement between the University of Alabama at Birmingham and Idera Pharmaceuticals, Inc.; funds from the University of Alabama at Birmingham Comprehensive Cancer Center for Cancer Pharmacology Laboratory, NIH grant P60 AR20614 (for the apoptosis analyses done by the Flow Cytometry Core of the Arthritis and Musculoskeletal Center); and a Predoctoral Traineeship Award from the Department of Defense Prostate Cancer Research Program grant W81XWH-06-1-0063 (E.R. Rayburn).

The costs of publication of this article were defrayed in part by the payment of page charges. This article must therefore be hereby marked advertisement in accordance with 18 U.S.C. Section 1734 solely to indicate this fact.

Requests for reprints: Ruiwen Zhang, Department of Pharmacology and Toxicology, University of Alabama at Birmingham, 1670 University Boulevard, 113 Volker Hall, Birmingham, AL 35294. Phone: 205-934-8558; Fax: 205-975-9330. E-mail: Ruiwen.Zhang@ccc.uab.edu

Copyright © 2006 American Association for Cancer Research.

doi:10.1158/1535-7163.MCT-06-0158

dinucleotide results in immune system stimulation (26, 27, 32). However, the sequences flanking the dinucleotide, the accessibility to the 5' end, and the presence of secondary structures also play a role (28–31). Moreover, recent studies have shown that TLR9 exhibits nucleotide motif recognition patterns and recognizes synthetic immunostimulatory dinucleotide motifs (32–34, 36). Agonists of TLR9-containing synthetic immunostimulatory motifs and novel DNA structures, called immunostimulatory oligonucleotides (IMO), have recently been reported. IMOs induce potent immune responses distinct from those induced by natural CpG-containing DNA (32–37).

We and others have previously shown that IMOs and CpG-containing oligonucleotides have antitumor effects against several different models of human cancer, including glioma, leukemia, sarcoma, and various other cancers (36–42). Because new therapeutic approaches for breast cancer are urgently needed and the IMO has been shown to have anticancer effects, we decided to evaluate whether it could be used as a new strategy for breast cancer therapy. Two human breast cancer cell lines were examined for effects on cell growth, proliferation, and apoptosis following exposure to the IMO. The best means for administration of the IMOs to optimize their therapeutic efficacy is also largely unknown; in the present study, we examined the pharmacokinetics and antitumor activity of an IMO containing a synthetic stimulatory motif (CpR, R is 2'-deoxy-7-deazaguanosine) and 3'-3'-linked DNA structure (32, 33, 43) in models of breast cancer. The 3'-3'-linked DNA structure increases the efficacy and the nuclease stability of the oligonucleotide, allowing it to remain in the bloodstream and tissues for a longer time than traditional oligonucleotides (29, 30, 43). An oligonucleotide with a similar structure but lacking an immunostimulatory dinucleotide motif was used as a control.

Materials and Methods

IMOs and Reagents

IMO, 5'-TCTGTCRTTCT-X-TCTTCTGTCT-5'; ³⁵S-IMO (specific activity, 213 μCi/mg); and a control nonstimulatory IMO, 5'-TCTCACCTTCT-X-TCTTCCACTCT-5' (where R and X stand for 2'-deoxy-7-deazaguanosine and a glycerol linker, respectively) with phosphorothioate backbones, were synthesized, purified, and analyzed as previously reported (44). The purity of the IMO was shown to be >90% by capillary gel electrophoresis and PAGE analyses, with the remainder being n-1 and n-2 products. The integrity of internucleotide linkages and molecular mass were confirmed by ³¹P nuclear magnetic resonance and matrix-assisted laser desorption/ionization–time of flight mass spectrophotometric analysis. The IMO and control oligonucleotide contained <0.2 EU/mL of endotoxin as determined by the *Limulus* assay (BioWhittaker, Inc., Walkersville, MD).

All chemicals and solvents were of the highest analytic grade available. Cell culture medium, fetal bovine serum, PBS, sodium pyruvate, nonessential amino acids, penicillin-streptomycin, and other cell culture supplies were

obtained from the Comprehensive Cancer Center Media Preparation Shared Facility, University of Alabama at Birmingham. Matrigel basement membrane matrix was obtained from Becton Dickinson Labware (Bedford, MA). Tissue solubilizer (TS-2) was purchased from Research Products, Inc. (Mt. Prospect, IL).

Cell Culture

The MCF-7, BT474, and MDA-MB-468 human breast cancer cell lines and the 4T1 murine mammary cell line were obtained from the American Type Culture Collection (Rockville, MD) and cultured according to the instructions from the manufacturer. MCF-7 cells were grown in Eagle's MEM supplemented with 2 mmol/L L-glutamine, 1.5 g/L sodium bicarbonate, 0.1 mmol/L nonessential amino acids, and 1 mmol/L sodium pyruvate. BT474 cells were grown in modified Dulbecco's medium. MDA-MB-468 cells were grown in Leibovitz's L-15 medium supplemented with 2 mmol/L L-glutamine. The 4T1 cells were grown in RPMI 1640 supplemented with 2 mmol/L glutamine, 1.5 g/L sodium bicarbonate, 4.5 g/L glucose, 10 mmol/L HEPES, and 1 mmol/L sodium pyruvate. All media contained 1% penicillin-streptomycin and 10% fetal bovine serum.

Animals

The animal use and care protocol was approved by the Institutional Animal Use and Care Committee of the University of Alabama at Birmingham. Female athymic pathogen-free nude mice (nu/nu, 4–6 weeks) were purchased from Frederick Cancer Research and Development Center (Frederick, MD). CD-1 mice (4–6 weeks) and BALB/c mice (6–8 weeks) were obtained from Charles River Laboratories (Cambridge, MA).

Tumor Models

Human cancer xenograft models were established using methods reported previously (44–46). When confluence reached 80%, cultured BT474 or 4T1 cells were harvested from the monolayer cultures, washed with serum-free medium, and resuspended at a ratio of 3:1 in the same medium with Matrigel basement membrane matrix, then injected s.c. (5×10^6 cells, total volume 0.2 mL) into the left inguinal area of nude mice (BT474) or BALB/c mice (4T1). To establish MCF-7 human breast cancer xenografts, each of the female nude mice was implanted with a 60-day s.c. slow release estrogen pellet (SE-121, 1.7 mg 17β-estradiol/pellet; Innovative Research of America, Sarasota, FL). Cultured MCF-7 cells were harvested from monolayer cultures, washed twice with serum-free medium, resuspended, and injected s.c. (5×10^6 cells, total volume 0.2 mL) into the left inguinal area of the mice. All animals were monitored for activity, physical condition, body weight, and tumor growth. Tumor size was determined by caliper measurement in two perpendicular diameters of the implant every other day. Tumor weight (in grams) was calculated by the formula, $1/2a \times b^2$, where a is the long diameter and b is the short diameter (in centimeters).

In vivo Treatment with the IMO Alone or in Combination with Herceptin

The animals bearing human cancer xenografts were randomly divided into various treatment groups and a

control group (5–10 mice/group). The untreated control group received physiologic saline (0.9% NaCl) only. The IMO dissolved in physiologic saline (0.9% NaCl) was administered by s.c. injection at doses of 0.5 or 1 mg/kg/d, three doses per week. The treatment schedule was as follows. For the MCF7 model, the IMO or the control oligonucleotide was administered by s.c. injection at a dose of 0.5 mg/kg three doses per week for 2 weeks when animals were observed to have established tumors of ~60 mg. For the BT474 model, the IMO or the control oligonucleotide were administered by s.c. injection at a dose of 1 mg/kg when established tumors were noted (tumor mass of ~90 mg, 1 week after cell injection), three doses per week for 6 weeks. Herceptin was administered i.p. at a dose of 1 mg/kg on days 4, 11, 18, and 25. For the 4T1 model, animals bearing 4T1 tumors were treated with 1 mg/kg of the IMO or the control oligonucleotide thrice per week for 2 weeks once established (~110 mg) tumors were present. Treatment was started at different tumor sizes for the different models to ensure that the xenograft tumors were well established and in the exponential growth phase.

Tissue Distribution of the IMO following Various Routes of Administration

Tissue distribution studies were accomplished using a protocol similar to that previously described (44) with mice in metabolism cages. An [³⁵S]-IMO (2 mg/kg, 2 μCi/mouse) was administered to CD-1 mice or nude mice bearing MCF7 xenografts (three animals for each time point) at a single dose of 2 mg/kg by various routes: s.c., i.v., p.o., or i.p. Blood and tissue samples were collected in heparinized tubes at 1, 4, and 24 hours after dosing. Plasma was separated by centrifugation at 20,000 × *g* for 5 minutes. Tissues, including the liver, kidneys, heart, lung, spleen, brain, and tumor, were taken at various times and immediately blotted on Whatman no. 1 filter paper, trimmed of extraneous fat and connective tissue, weighed, and homogenized in physiologic saline (0.9% NaCl; 5 mL/g wet weight). The resulting homogenates were stored at -70°C until further analysis. The total radioactivity of IMO in tissues and body fluids was determined by liquid scintillation spectrometry (LS 6000T A; Beckman, Irvine, CA), using a method described previously (46). In brief, plasma samples (50 μL) were mixed with 5 mL of scintillation solvent (Beckman). Tissue homogenates (50–200 μL) were mixed with 200 μL solubilizer (TS-2) overnight, neutralized with 400 μL of 0.3% acetic acid, and then mixed with scintillation solvent (5 mL) before analysis. The radioactivity was quantified in triplicate for each sample and the levels of radioactivity-derived IMO in biological fluids and tissues were expressed as means ± SE of the results from at least three animals for each time point.

Determination of Cell Survival *In vitro*

The percentage of cell survival was determined by using the 3-(4,5-dimethylthiazol-2-yl)-2,5-diphenyltetrazolium bromide assay as previously reported (45, 46). MCF-7

and MDA-MB-468 cells were grown in 96-well plates and exposed for 48 hours to the IMO or control oligonucleotide (0, 1, 5, 10, 50, and 100 nmol/L) with or without Lipofectin (Life Technologies; Gaithersburg, MD; 7 μg/mL). The percentage of cell survival was calculated by dividing the mean absorbance of wells containing treated cells by that of untreated control wells.

Detection of Apoptosis

IMO-treated and control oligonucleotide-treated and untreated control cells in early and late stages of apoptosis were detected using an Annexin V-FITC apoptosis detection kit from BioVision (Mountain View, CA; refs. 45, 46). Cells were transfected with the IMO (100 nmol/L) or the control oligonucleotide (100 nmol/L) with or without Lipofectin and incubated for 24 hours before analysis. Media and cells were collected and washed with serum-free medium. Cells that were positive for Annexin V-FITC alone (early apoptosis) and Annexin V-FITC and propidium iodide (late apoptosis) were counted, and the apoptotic index was calculated.

Evaluation of Cell Proliferation

Proliferation was evaluated using a cell proliferation kit from Oncogene (La Jolla, CA; refs. 45, 46). Cells were seeded in 96-well plates and transfected with the IMO (100 nmol/L) or the control IMO (100 nmol/L) for 24 hours, and then BrdUrd was added to the medium 10 hours before treatment termination. The level of BrdUrd incorporated into cells was quantified by anti-BrdUrd antibody, and absorbance was measured at dual wavelengths (450/540 nm).

Data and Statistical Analysis

The antitumor activity (as measured by differences in tumor mass) was expressed as mean and SD values. The significance of differences was analyzed by ANOVA or Student's *t* test as appropriate.

Results

The IMO Is Distributed to Various Tissues

The tissue distribution of the IMO administered by different routes in mice was first evaluated in normal CD-1 mice. The animals were given ³⁵S-IMO at a single dose of 2 mg/kg (2 μCi/mouse) by various routes, s.c., i.v., i.p., and p.o., and the IMO concentration in blood and tissue samples was quantified by measuring ³⁵S-derived radioactivity. There are significant differences in tissue uptake of IMO following various routes of administration (Fig. 1, *P* < 0.001). At the test dose level, the IMO was detectable in various tissues at 1 hour (Fig. 1A) after administration, 4 hours (Fig. 1B) after, and up to 24 hours (Fig. 1C) after administration, indicating the prolonged circulation and retention of the IMO. After administration by i.v., i.p., and s.c. routes, the highest IMO levels were seen in liver, kidney, and spleen, with modest levels in lung and heart. Although i.v. injection resulted in a higher concentration at 1 hour after dosing, comparable concentrations were seen for all the routes. Interestingly, the IMO was detected in all test tissues

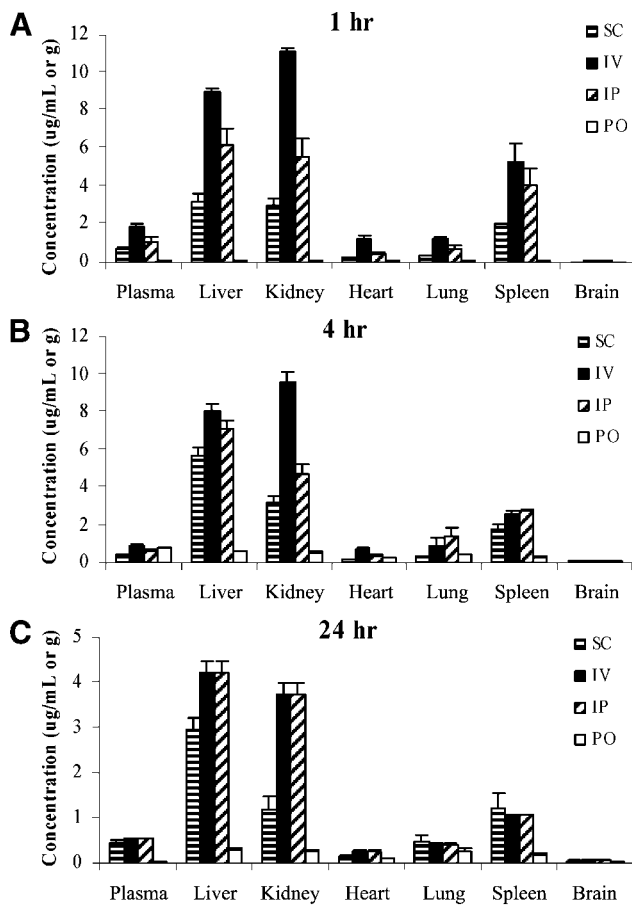


Figure 1. Distribution of the IMO in CD-1 mice. Plasma and tissue samples were collected 1 (A), 4 (B), and 24 (C) h after administration of the ^{35}S -IMO (2 mg/kg, 2 $\mu\text{Ci}/\text{mouse}$) by the s.c., i.v., i.p. and p.o. routes, and the amount of IMO in the samples was quantitated by liquid scintillation spectrometry.

(nongastrointestinal tract tissues) at all time points after p.o. administration, indicating that the IMO was p.o. bioavailable (Fig. 1). Of note, the pattern of tissue distribution after p.o. administration was different from other routes, more evenly distributed in the various tissues.

The IMO Is Taken Up by Tumor Tissues

The tissue distribution pattern after i.v. and s.c. administration was further compared in nude mice bearing MCF7 xenograft tumors. The tumor-bearing mice were administered the same dose of ^{35}S -IMO by s.c. and i.v. injection. Both routes of administration showed similar tissue distribution of the IMO both 1 hour (Fig. 2A) and 24 hours (Fig. 2B) after administration. Interestingly, the s.c. administration route increased the concentration of IMO within the tumor compared with i.v. administration. Because s.c. administration provided a favorable tissue distribution pattern, prolonged retention time, and a high concentration of the IMO within the tumor, we used this route of administration in subsequent *in vivo* efficacy studies.

The IMO Has Activity against Human Breast Cancer in Xenograft Models

We generated two xenograft models of human breast cancer to test the IMO. Both the MCF7 and BT474 xenograft tumors showed decreased growth following administration of the IMO. In the MCF7 model, tumor growth was inhibited by 40% on day 18 ($P < 0.05$; Fig. 2C) in animals receiving IMO treatment at the low (0.5 mg/kg) dose level. The control oligonucleotide had no effect on tumor growth (Fig. 2C). In the BT474 model, tumor growth on day 70 in the IMO-treated (1 mg/kg) animals was inhibited by 67% compared with the saline-treated controls ($P < 0.05$; Fig. 3A). The control oligonucleotide showed a lesser

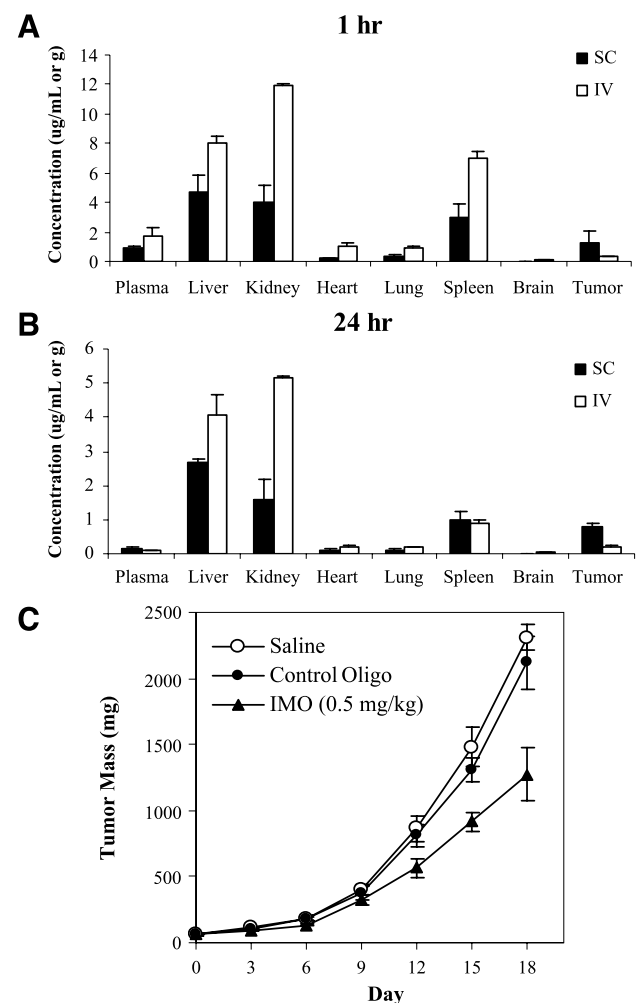


Figure 2. Distribution and *in vivo* anticancer activity of IMO nude mice bearing MCF-7 xenograft tumors. Tissue and plasma samples were collected 1 (A) and 24 (B) h after administration of the IMO (^{35}S -IMO, 2 mg/kg, 2 $\mu\text{Ci}/\text{mouse}$) to mice bearing MCF-7 tumors by the s.c. and i.v. routes, and the amount of IMO in the samples was quantitated by liquid scintillation spectrometry. The IMO, but not the control oligonucleotide (*oligo*), inhibited the growth of MCF-7 tumors (C) at lower dose of IMO (0.5 mg/kg, $P < 0.05$). Treatment was initiated after established tumors were present; and IMO or control oligonucleotide was given on days 0, 4, 7, 9, and 11.

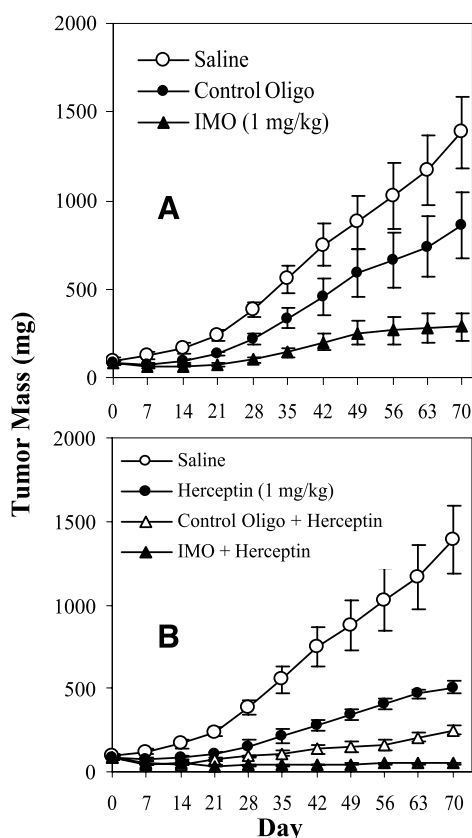


Figure 3. The IMO inhibits the growth of BT474 xenograft tumors and potentiates the effects of Herceptin. Mice bearing BT474 tumors were treated with the IMO or control oligonucleotide (A). The IMO and control oligonucleotide were evaluated in combination with Herceptin (B). Treatment was initiated after established tumors were observed (day 0). The IMO or control oligonucleotide was given s.c. at 1 mg/kg, thrice per week for 6 wks; Herceptin was administered i.p. at 1 mg/kg on days 4, 11, 18, and 25. IMO showed significant antitumor activity alone or in combination with Herceptin ($P < 0.05$).

effect. The growth inhibition of the MCF7 xenograft tumors by the IMO is remarkable, because a lower dose of the IMO (0.5 mg/kg; Fig. 2C) was used than the 1.0 mg/kg IMO used in the BT474 model (Fig. 3A). This suggests that even low doses of the IMO can bring about an antitumor response.

The IMO Enhances the Efficacy of the Anticancer Antibody Herceptin

Combining the IMO with Herceptin to treat mice bearing BT474 breast cancer xenograft tumors led to a significant inhibition of tumor growth (Fig. 3B). On day 70, the mean tumor size of the animals treated with both Herceptin and the IMO was 3.5% of that of the control animals treated with saline, whereas the mean tumor sizes for animals treated with the IMO or Herceptin alone were 21% and 36% of that of the control, respectively ($P < 0.01$; Fig. 3B). This represents a 6- to 10-fold increase in therapeutic effectiveness. Combination with the IMO did not change the toxicity profile of Herceptin (data not shown).

The IMO Has Antitumor Activity against Murine Syngeneic Graft Tumors

Xenograft models are frequently used to evaluate new anticancer agents, and the IMO is effective in both human and murine systems (34). To study the effects of the IMO in immunocompetent mice, we used the 4T1 syngeneic tumor model to verify the effects of the IMO seen in xenograft models. Mice bearing 4T1 tumors were treated with 1 mg/kg of the IMO or control oligonucleotide. Compared with the saline control group, the IMO inhibited tumor growth (Fig. 4). The IMO inhibited growth by 45% on day 18, whereas the control oligonucleotide inhibited tumor growth by 28% ($P < 0.05$). This shows that the IMO is effective in both nude and wild-type mouse models.

The IMO Decreases Cell Survival and Proliferation, and Increases Apoptosis in Human Breast Cancer Cell Lines

To determine whether the IMO has effects against breast cancer cells *in vitro*, cells were treated with the IMO or the control oligonucleotide and evaluated for cell survival, proliferation, and apoptosis. After transfection with Lipofectin, the IMO decreased the survival of MCF-7 and MDA-MB-468 cells by 60% and 46%, respectively ($P < 0.01$ and $P < 0.05$; Fig. 5A and D). IMO treatment also led to an increase in apoptosis in both cell lines, resulting in a >50% increase in apoptosis in the MCF-7 line ($P < 0.01$; Fig. 5B), and a >20% increase in the MDA-MB-468 cell line ($P < 0.05$; Fig. 5E). IMO treatment also decreased the proliferation of MCF-7 cells ($P < 0.05$; Fig. 5C). The MDA-MB-468 cells were less sensitive to the IMO (Fig. 5F). In both cell lines, the control oligonucleotide had little effect on cell survival, apoptosis, and proliferation than the IMO. Of note, with respect to induction of apoptosis

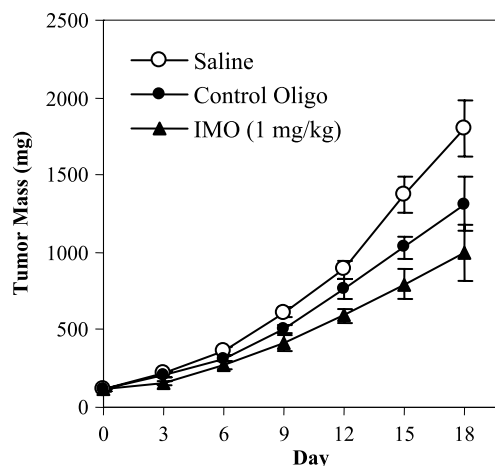
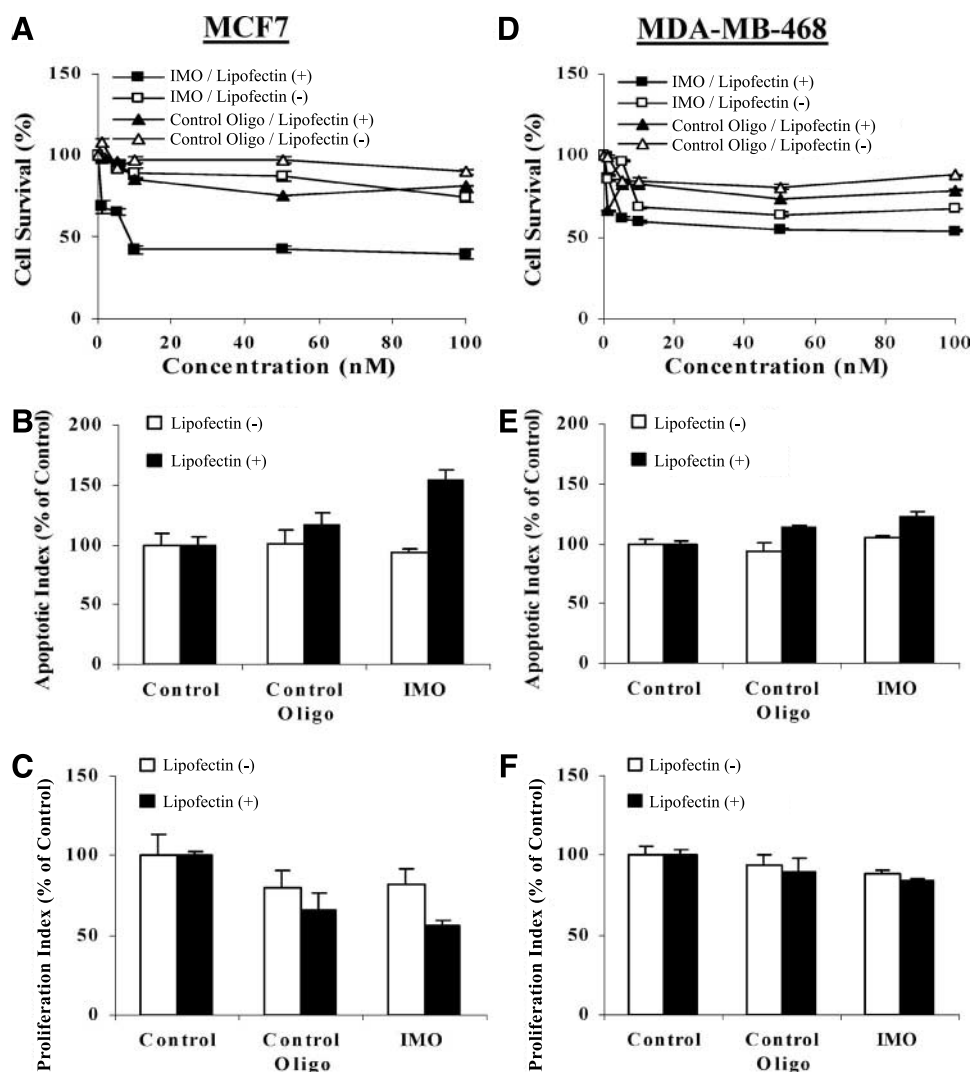


Figure 4. The IMO inhibits the growth of syngeneic 4T1 tumors. Mice bearing 4T1 tumors were treated with 1 mg/kg of the IMO or the control oligonucleotide thrice per week for 2 wks once established (~110 mg) tumors were present. The IMO showed significant anticancer activity ($P < 0.05$).

Figure 5. The IMO decreases survival (A and D), increases apoptosis (B and E), and decreases proliferation (C and F) in MCF-7 (A–C) and MDA-MB-468 (D–F) human breast cancer cell lines. The effects of IMO were determined in the presence and absence of Lipofectin. Lipofectin increased the IMO effects [$P < 0.05$, Lipofectin (+) versus Lipofectin (-)].



(Fig. 5B and E), the IMO had no effects when cells were exposed to the IMO without Lipofectin in both cell lines ($P < 0.05$). In cell proliferation assays, although both cell lines still showed a small effect when exposed to the IMO alone, the effect was increased in the presence of Lipofectin ($P < 0.05$; Fig. 5C and F). Similar potentially non-specific effects have been reported with Lipofectamine and other lipid agents with CpG and non-CpG oligonucleotides.

Discussion

Significant progress has been made in the design and development of TLR9 agonists in recent years. With increased understanding of the localization, signaling, and structure of TLR9 (47–49), designing better agonists and more effectively administering these agents to cell cultures, animal models, and human patients had become possible. As part of this progress, novel TLR9 agonists

containing synthetic dinucleotides and altered backbone structures (including a 3'-3'-linked structure) have been designed (32, 33, 35, 43). These IMOs have been shown to be more stable and induce a distinct immune response compared to traditional linear CpG oligos (33–36, 43). This second generation of TLR9 agonists has the potential to treat an astonishing range of human diseases, including infections, asthma, allergies, and cancer (33, 37, 50–54).

For various reasons, including the heterogeneity of tumors and the previous lack of knowledge about specific molecular targets, cytotoxic chemotherapy has remained a staple for the treatment of breast and other cancers since the introduction of 5-fluorouracil more than half a century ago. There have been recent additions to the arsenal being used to treat breast cancer, including antibodies and small-molecule inhibitors of specific receptors; however, there has not yet been a significant decrease in the incidence or mortality of the disease. Immunotherapy may be able to fill

the gaps left by the current therapeutic options. Although they cause specific antitumor effects, IMOs do not rely on specific gene products, or on the tissue type, to bring about antitumor effects. Activation of TLRs has shown potential for cancer treatment. For example, Aldara, a small molecule agonist of TLR7 has been approved for treatment of basal cell carcinoma. It is known that IMOs induce innate and adaptive immune responses through TLR9 activation, leading to various antitumor effects (38, 39, 52, 53). TLR9 agonism has also been suggested to have a number of effects on the tumor microenvironment and on signaling between the tumor, the immune system, and various other cells (13, 53, 54). In fact, TLR9 stimulation has been shown to decrease epidermal growth factor receptor signaling and angiogenesis (54). There is increasing evidence that TLR9 expression is not confined to immune cells (55–57). These studies suggest a role for TLR9 in tumor cells. TLR2 agonism has been shown to increase apoptosis; a similar effect may occur upon TLR9 stimulation (58). Although we have seen an increase in apoptosis *in vitro* when the IMO was administered with Lipofectin, the effects of TLR9 agonism on *in vivo* tumors remain to be examined. Many of the effects described could lead to tumor growth inhibition and/or mediate destruction of both the primary tumor and distant metastases.

Although IMOs have already been shown to stimulate the immune system, detailed studies of their pharmacokinetics have not previously been accomplished. As part of this study, we evaluated the tissue distribution of the IMO administered by various routes. We found that the IMO was widely distributed to a number of tissues, with the highest concentrations reaching the liver, kidneys, and spleen. The four main routes of administration (s.c., i.v., i.p., and p.o.) were evaluated, and all routes led to a similar distribution of the IMO. Additionally, we examined the distribution of the IMO to tissues in animals bearing MCF-7 xenograft tumors. We found that the IMO was again distributed to various tissues as well as to the tumor, with the s.c. route giving a high concentration of the IMO even 24 hours after administration, providing a basis for further efficacy testing *in vivo*, including other animal models and human clinical trials. In addition, the p.o. bioavailability of the IMO provides a new avenue for the development of IMOs as p.o. therapeutic agents. The results with p.o. administration are in agreement with previous studies of antisense oligonucleotides (44, 59) that show that antisense oligonucleotides with advanced chemistry can be absorbed and exert antitumor activity after p.o. administration. Although we cannot discount the possibility that some of the radioactivity detected may be associated with products of metabolism, based on our previous studies with ³⁵S-labeled oligonucleotides, it is unlikely that free ³⁵S was taken up by the tumor and tissues. Further, IMOs have previously been shown to be stable for up to 48 hours in cell culture (with serum; ref. 43). Therefore, due to the fact that most oligonucleotides are degraded from the 3' end and that the novel IMO has a 3'-3' linker, preventing extensive degradation

by nucleases, and that the IMO is labeled on its 5' end (which is the last part of the molecule to be degraded; ref. 43), it is most likely that the ³⁵S-labeled molecule detected was the IMO.

We evaluated the IMO in two xenograft models of human breast cancer and a syngeneic model of murine mammary cancer. Although nude mouse xenograft models are widely accepted for studying cancer therapeutic molecules, we examined the effects of the IMO in a syngeneic model to study the antitumor effect in mice with a normal immune system. Additionally, it could be suggested that nude mouse models do not represent an appropriate model for studying an immunotherapeutic molecule due to their immunocompromised state. This could lead to underestimation of the effects of the IMO. However, we and others have previously studied the effects of IMOs and immunostimulatory oligonucleotides in nude mice, and have observed potent antitumor effects. This may be due to the fact that nude mice do still possess macrophages, B cells and natural killer cells. Both B cells and natural killer cells are known to express TLR9 (38).

In the present study, we also showed that the IMO decreases cell survival and proliferation, and increases apoptosis in breast cancer cell lines *in vitro*. However, these effects were only observed when the cells were transfected with Lipofectin (to facilitate internalization of the IMO). It has been suggested that TLR9 is located intracellularly, setting it apart from other TLRs, which are usually located on the cell surface. Our data support the notion that IMO recognition by and interaction with TLR9 are most likely to occur inside the cell. Although both cell lines responded to the IMO, they were not affected equally. It is not clear what mechanism(s) are responsible for the differences of MCF-7 and MDA-MB-468 cells. Both of the cell lines express similar levels of TLR9.⁵ There are a few major differences in the genetic background of the two cell lines, including p53 status and estrogen receptor- α status, there may also be differences in the expression of required downstream signaling molecules, such as MyD88. The role of both of these molecules in IMO-mediated cell growth inhibition and induction of apoptosis should be further examined in future investigations. Additionally, although Lipofectin is necessary for there to be significant effects *in vitro*, the IMO can be effective *in vivo* when administered without any delivery system. The mechanism by which internalization occurs *in vivo* is still unknown, but a similar effect is seen when antisense oligonucleotides are used (60).

Demonstrating the broad applicability of the IMO, we noted that the IMO was effective in models of breast cancer with different genetic backgrounds. The IMO showed potent anti-breast cancer effects *in vitro* and *in vivo* against estrogen receptor-positive (MCF-7) and estrogen receptor-negative (BT4747, MDA-MB-468) cells

⁵H. Wang et al., unpublished data.

and tumors, against ErbB2-overexpressing (BT474) and ErbB2-negative (MCF-7, MDA-MB-468) cells and tumors, and against p53 wild-type (MCF-7) and mutant (BT474, MDA-MB-468) tumors, as well as against both xenograft and syngeneic (4T1) tumors. These data suggest that although there were differences in the responsiveness of different cancer cell lines, the IMO is still effective against a variety of tumors with different genetic backgrounds.

Most cancer therapy now relies on a combination of agents, so we also evaluated the IMO in combination with Herceptin (trastuzumab), targeting ErbB2, which is over-expressed in ~30% of breast cancers (61). Herceptin is thought to work by decreasing expression of the receptor (thereby decreasing growth), by down-regulation of angiogenic factors, and by antibody-dependent cell cytotoxicity (62). Because the IMO stimulates the innate immune system, it is logical that it may also increase the efficacy of antibodies by increasing the likelihood that the antibody complexes will be recognized by the host immune system. We noted significant tumor growth inhibition and a 6- to 10-fold increase in the therapeutic efficacy of Herceptin, with no change in the toxicity of either agent. This increase in efficacy could be due to increased immune system recognition of the tumor, by antibody-dependent cell cytotoxicity, or by other pathways, such as inhibition of angiogenesis. Combining the IMO with other antibodies, chemotherapy or radiation therapy would also likely lead to an increase in the therapeutic efficacy of these agents. In addition to the effects mentioned above, combining the IMO with other therapeutic modalities could lead to other antitumor effects. Future studies will examine both combining the IMO with other therapeutic modalities and the mechanism(s) responsible for any resulting antitumor effects. We also did not examine the different supporting structures or substructures of breast tumors in the present study. Given the importance of these structures (particularly the stroma) for breast cancer, it may be of interest for future studies to examine whether there are differences in stromal/epithelial signaling following treatment with the IMO, or to determine whether there are differences in the uptake or effects of the IMO.

In conclusion, this is the first comprehensive report of the tissue distribution of the IMO following administration by various routes. The IMO led to strong anticancer effects and potentiated the effects of an anticancer antibody. These results indicate that the IMO would be an effective candidate for clinical use against breast cancer either alone or in combination with other agents.

Acknowledgments

We thank Drs. Robert B. Diasio and Donald L. Hill for helpful discussions.

References

1. American Cancer Society. Cancer facts and figures 2006. Atlanta (Georgia): American Cancer Society; 2006.
2. National Cancer Institute. NCI fact book. Bethesda (Maryland): National

Cancer Institute; 2004. Available from <http://www3.cancer.gov/admin/fmb/2003factbook.pdf>.

3. American Cancer Society. Surveillance research, 2006. Age-adjusted cancer death rates, females by site, 1930-2002. Atlanta (Georgia): American Cancer Society; 2006.
4. Rutqvist LE, Johansson H, Signomkiao T, Johansson U, Fornander T, Wilking N. Adjuvant tamoxifen therapy for early stage breast cancer and second primary malignancies. *J Natl Cancer Inst* 1995;87:645–51.
5. Nicholson RI, Johnston SR. Endocrine therapy—current benefits and limitations. *Breast Cancer Res Treat* 2005;93 Suppl 1:S3–10.
6. Zhou J, Zhong Y. Breast cancer immunotherapy. *Cell Mol Immunol* 2004;1:247–55.
7. Yamamoto S, Kuramoto E, Shimada S, Tokunaga T. *In vitro* augmentation of natural killer cell activity and production of interferon- α/β and γ with deoxyribonucleic acid fraction from *Mycobacterium bovis* BCG. *Jpn J Cancer Res* 1988;79:866–73.
8. Tokunaga T, Yano O, Kuramoto E, et al. Synthetic oligonucleotides with particular base sequences from the cDNA encoding proteins of *Mycobacterium bovis* BCG induce interferons and activate natural killer cells. *Microbiol Immunol* 1992;36:55–66.
9. Kataoka T, Yamamoto S, Yamamoto T, et al. Antitumor activity of synthetic oligonucleotides with sequences from cDNA encoding proteins of *Mycobacterium bovis* BCG. *Jpn J Cancer Res* 1992;83:244–7.
10. Tokunaga T, Yamamoto T, Yamamoto S. How BCG led to the discovery of immunostimulatory DNA. *Jpn J Infect Dis* 1999;52:1–11.
11. Hemmi H, Takeuchi O, Kawai T, et al. A Toll-like receptor recognizes bacterial DNA. *Nature* 2000;408:740–5.
12. Janeway CA, Jr., Medzhitov R. Innate immune recognition. *Annu Rev Immunol* 2002;20:197–216.
13. Takeshita F, Gursel I, Ishii KJ, Suzuki K, Gursel M, Klinman DM. Signal transduction pathways mediated by the interaction of CpG DNA with Toll-like receptor 9. *Semin Immunol* 2004;16:17–22.
14. Messina JP, Gilkeson GS, Pisetsky DS. Stimulation of *in vitro* murine lymphocyte proliferation by bacterial DNA. *J Immunol* 1991;147:1759–64.
15. Yamamoto S, Yamamoto T, Kataoka T, Kuramoto E, Yano O, Tokunaga T. Unique palindromic sequences in synthetic oligonucleotides are required to induce IFN and augment IFN-mediated natural killer activity. *J Immunol* 1992;148:4072–6.
16. Klinman DM, Yi AK, Beaucage SL, Conover J, Kreig AM. CpG motifs present in bacteria DNA rapidly induce lymphocytes to secrete interleukin 6, interleukin 12, and interferon γ . *Proc Natl Acad Sci U S A* 1996;93:2879–83.
17. Warren TL, Bhatia SK, Acosta AM, et al. APC stimulated by CpG oligodeoxynucleotide enhance activation of MHC class I-restricted T cells. *J Immunol* 2000;165:6244–51.
18. Chu RS, Askew D, Noss EH, Tobian A, Krieg AM, Harding CV. CpG oligodeoxynucleotides down-regulate macrophage class II MHC antigen processing. *J Immunol* 1999;163:1188–94.
19. Zhao Q, Tamsamani J, Zhou RZ, Agrawal S. Pattern and Kinetics of cytokine production following administration of phosphorothioate oligonucleotides in mice. *Antisense Nucleic Acid Drug Dev* 1997;7:495–502.
20. Sabroe I, Parker LC, Wilson AG, Whyte MK, Dower SK. Toll-like receptors: their role in allergy and non-allergic inflammatory disease. *Clin Exp Allergy* 2002;32:984–9.
21. Van Uden J, Raz E. Immunostimulatory DNA and applications to allergic disease. *J Allergy Clin Immunol* 1999;104:902–10.
22. Dalpke A, Zimmermann S, Heeg K. CpG DNA in the prevention and treatment of infections. *BioDrugs* 2002;16:419–31.
23. Cafaro A, Titti F, Fracasso C, et al. Vaccination with DNA containing tat coding sequences and unmethylated CpG motifs protects cynomolgus monkeys upon infection with simian/human immunodeficiency virus (SHIV89.6P). *Vaccine* 2001;6:2862–77.
24. Carpentier AF, Xie J, Mokhtari K, Delattre JY. Successful treatment of intracranial gliomas in rat by oligodeoxynucleotides containing CpG motifs. *Clin Cancer Res* 2002;6:2469–73.
25. Ikeda H, Chamoto K, Tsuji T, et al. The critical role of type-1 innate and acquired immunity in tumor immunotherapy. *Cancer Sci* 2004;95:697–703.
26. Zhao Q, Yu D, Agrawal S. Immunostimulatory activity of CpG

- containing phosphorothioate oligodeoxynucleotide is modulated by modification of a single deoxynucleoside. *Bioorg Med Chem Lett* 2000;10:1051–4.
27. Yu D, Kandimalla ER, Zhao Q, Cong Y, Agrawal S. Modulation of immunostimulatory activity of CpG oligonucleotides by site-specific deletion of nucleobases. *Bioorg Med Chem Lett* 2001;11:2263–7.
28. Zhao Q, Tamsamani J, Iadarola PL, Jiang Z, Agrawal S. Effect of different chemically modified oligodeoxynucleotides on immune stimulation. *Biochem Pharmacol* 1996;51:173–82.
29. Yu D, Zhao Q, Kandimalla ER, Agrawal S. Accessible 5'-end of CpG-containing phosphorothioate oligodeoxynucleotides is essential for immunostimulatory activity. *Bioorg Med Chem Lett* 2000;10:2585–8.
30. Kandimalla ER, Bhagat L, Yu D, Cong Y, Tang J, Agrawal S. Conjugation of ligands at the 5'-end of CpG DNA affects immunostimulatory activity. *Bioconjug Chem* 2002;13:966–74.
31. Yu D, Kandimalla ER, Zhao Q, Bhagat L, Cong Y, Agrawal S. Requirement of nucleobase proximal to CpG dinucleotide for immunostimulatory activity of synthetic CpG DNA. *Bioorg Med Chem* 2003;11:459–64.
32. Kandimalla ER, Yu D, Zhao Q, Agrawal S. Effect of chemical modifications of cytosine and guanine in a CpG-motif of oligonucleotides: structure-immunostimulatory activity relationships. *Bioorg Med Chem* 2001;9:807–13.
33. Kandimalla ER, Bhagat L, Wang D, et al. Divergent synthetic nucleotide motif recognition pattern: design and development of potent immunomodulatory oligodeoxynucleotide agents with distinct cytokine induction profiles. *Nucleic Acids Res* 2003;31:2393–400.
34. Kandimalla ER, Bhagat L, Zhu FG, et al. A dinucleotide motif in oligonucleotides shows potent immunomodulatory activity and overrides species-specific recognition observed with CpG motif. *Proc Natl Acad Sci U S A* 2003;100:14303–8.
35. Kandimalla ER, Yu D, Agrawal S. Towards optimal design of second-generation immunomodulatory oligonucleotides. *Curr Opin Mol Ther* 2002;4:122–9.
36. Kandimalla ER, Bhagat L, Li Y, et al. Immunomodulatory oligonucleotides containing a cytosine-phosphate-2'-deoxy-7-deazaguanosine motif as potent toll-like receptor 9 agonists. *Proc Natl Acad Sci U S A* 2005;102:6925–30.
37. Wang D, Li Y, Yu D, Song SS, Kandimalla ER, Agrawal S. Immunopharmacological and antitumor effects of second-generation immunomodulatory oligonucleotides containing synthetic CpR motifs. *Int J Oncol* 2004;24:901–8.
38. Wang H, Rayburn E, Zhang R. Synthetic oligodeoxynucleotides containing deoxycytidyl-deoxyguanosine dinucleotides (CpG ODNs) and modified analogs as novel anticancer therapeutics. *Curr Pharm Des* 2005;11:2889–907.
39. Krieg AM. Antitumor applications of stimulating toll-like receptor 9 with CpG oligodeoxynucleotides. *Curr Oncol Rep* 2004;6:88–95.
40. Wooldridge JE, Weiner GJ. CpG DNA and cancer immunotherapy: orchestrating the antitumor immune response. *Curr Opin Oncol* 2003;15:440–5.
41. Carpentier AF, Auf G, Delattre JY. CpG-oligonucleotides for cancer immunotherapy: review of the literature and potential applications in malignant glioma. *Front Biosci* 2003;8:e115–27.
42. Weiner GJ. The immunobiology and clinical potential of immunostimulatory CpG oligodeoxynucleotides. *J Leukoc Biol* 2003;68:455–63.
43. Yu D, Kandimalla ER, Bhagat L, Tang JY, Cong Y, Agrawal S. "Immunomers"—novel 3'-3'-linked CpG oligodeoxynucleotides as potent immunomodulatory agents. *Nucleic Acids Res* 2002;30:4460–9.
44. Wang H, Cai Q, Zeng X, Yu D, Agrawal S, Zhang R. Antitumor activity and pharmacokinetics of a mixed-backbone antisense oligonucleotide targeted to the R1 α subunit of protein kinase A after oral administration. *Proc Natl Acad Sci U S A* 1999;96:13989–94.
45. Zhang Z, Li M, Wang H, Agrawal S, Zhang R. Antisense therapy targeting MDM2 oncogene in prostate cancer: Effects on proliferation, apoptosis, multiple gene expression, and chemotherapy. *Proc Natl Acad Sci U S A* 2003;100:11636–41.
46. Wang H, Yu D, Agrawal S, Zhang R. Experimental therapy of human prostate cancer by inhibiting MDM2 expression with novel mixed-backbone antisense oligonucleotides: *in vitro* and *in vivo* activities and mechanisms. *Prostate* 2003;54:194–205.
47. Nishiya T, DeFranco AL. Ligand-regulated chimeric receptor approach reveals distinctive subcellular localization and signaling properties of the Toll-like receptors. *J Biol Chem* 2004;279:19008–17.
48. Barton GM, Kagan JC, Medzhitov R. Intracellular localization of Toll-like receptor 9 prevents recognition of self DNA but facilitates access to viral DNA. *Nat Immunol* 2006;7:49–56.
49. Latz E, Visintin A, Espevik T, Golenbock DT. Mechanisms of TLR9 activation. *J Endotoxin Res* 2004;10:406–12.
50. Zhu FG, Kandimalla ER, Yu D, Tang JX, Agrawal S. Modulation of ovalbumin-induced Th2 responses by second-generation immunomodulatory oligonucleotides in mice. *Int Immunopharmacol* 2004;4:851–62.
51. Li Y, Kandimalla ER, Yu D, Agrawal S. Oligodeoxynucleotides containing synthetic immunostimulatory motifs augment potent Th1 immune responses to HBsAg in mice. *Int Immunopharmacol* 2005;5:981–91.
52. Saha A, Baral RN, Chatterjee SK, et al. CpG oligonucleotides enhance the tumor antigen-specific immune response of an anti-idiotypic antibody-based vaccine strategy in CEA transgenic mice. *Cancer Immunol Immunother* 2006;55:515–27.
53. Guiducci C, Vicari AP, Sangaletti S, Trinchieri G, Colombo MP. Redirecting *in vivo* elicited tumor infiltrating macrophages and dendritic cells towards tumor rejection. *Cancer Res* 2005;65:3437–46.
54. Damiano V, Caputo R, Bianco R, et al. Novel Toll-like receptor 9 agonist induces epidermal growth factor receptor (EGFR) inhibition and synergistic antitumor activity with EGFR inhibitors. *Clin Cancer Res* 2006;12:577–83.
55. Nishimura M, Naito S. Tissue-specific mRNA expression profiles of human toll-like receptors and related genes. *Biol Pharm Bull* 2005;28:886–92.
56. Droemann D, Albrecht D, Gerdes J, et al. Human lung cancer cells express functionally active Toll-like receptor 9. *Respir Res* 2005;6:1.
57. Pratesi G, Petrangolini G, Tortoreto M, et al. Therapeutic synergism of gemcitabine and CpG-oligodeoxynucleotides in an orthotopic human pancreatic carcinoma xenograft. *Cancer Res* 2005;65:6388–93.
58. Aliprantis AO, Yang RB, Weiss DS, Godowski P, Zychlinsky A. The apoptotic signaling pathway activated by Toll-like receptor-2. *EMBO J* 2000;19:3325–36.
59. Agrawal S, Zhang X, Zhao H, et al. Absorption, tissue distribution and *in vivo* stability in rats of a hybrid antisense oligonucleotide following oral administration. *Biochem Pharm* 1995;50:571–6.
60. Dean NM, Bennett CF. Antisense oligonucleotide-based therapeutics for cancer. *Oncogene* 2003;22:9087–96.
61. Foster CS, Gosden CM, Ke Y. HER2/neu expression in cancer: the pathologist as diagnostician or prophet? *Hum Pathol* 2003;34:635–8.
62. Nahta R, Esteva FJ. HER-2-targeted therapy: lessons learned and future directions. *Clin Cancer Res* 2003;9:5078–84.